Mathematical Geology, Vol. 22, No. 1, 1990

Variance as a Function of Sample Support Size[1]

R. Zhang,[2] A. W. Warrick,[2] and D. E. Myers[3]

The effect of sample support size on variance is examined and evaluated. Results based on variograms and geostatistics are compared to the classical relationship developed by H. F. Smith in 1938; that is, that the variance is reduced from V_1 *to* V_1/n^b *as the support area increases from 1 to* n *plots for uniformity trials. The exponent* b *is between zero and one. Theoretical results are based on use of auxiliary functions and account for the size and shape of the sample support and the overall field geometry. Results are given in terms of approximations by rational functions for ease of calculation. Experimental results for uniformity trials, infiltration measurements, and spectral data from satellites are compared to theoretical and empirical results. Applications include not only uniformity trials, but also measurement theory.*

KEY WORDS: Variogram, geostatistics, sample support, variance

INTRODUCTION

Sample support size is of fundamental importance for various measurement and estimation problems. For example, sensor geometry, comparisons of alternative measurement devices, and plot size determination, all require examination of the variability of results as influenced by dimensions of the samples. Smith (1938) presented an empirical law relating variance of crop yield per unit area to plot size:

$$V_n = V_1/n^b \tag{1}$$

where V_n is the variance among plots, each with an area of n units and V_1 is the variance among plots, each of unit size. Factor "b" is an index of heterogeneity between 0 and 1. If sampling is random, b will be 1. However, if sampling is not random, b will be less than 1 and could approach zero if no heterogeneity exists. If n corresponds to an area W and the unit support size is w, Eq. (1) is equivalent to

$$V_W = V_w[w/W]^b \tag{2}$$

with V_W and V_w corresponding to the variances of the two areas.

[1]Manuscript received 29 March 1989; accepted 7 July 1989.

[2]Department of Soil and Water Science, University of Arizona, Tucson, Arizona 85721, U.S.A.

[3]Department of Mathematics, University of Arizona, Tucson, Arizona 85721, U.S.A.

0882-8121/90/0100-0107S06.00/1

An alternative approach to quantification of heterogeneity is through geostatistics. Our primary objective is to evaluate variance as a function of sample support. A second objective is to relate the empirical index of heterogeneity b of Eq. (1) to variograms. Previous results along these lines are given in Whittle (1956) and Starks (1986).

THEORY

The variogram $\gamma(h)$ is defined as (cf. Journel and Huijbregts, 1978)

$$\gamma(h) = (1/2)\ \mathrm{Var}\left[Z(x) - Z(x + h)\right] \tag{3}$$

with "Var" the variance of the argument. In this discussion, the intrinsic hypothesis is assumed; that is, the expected value of $Z(x)$ is independent of any point x, or

$$E\left[Z(x)\right] = \mu \tag{4}$$

and γ is a function of h only as implied in Eq. (3). (For some examples, second-order stationarity will be assumed, which implies the existence of a finite population variance σ^2.) Only isotropic models will be considered.

Curve I (Fig. 1) shows a typical spherical variogram starting at $\gamma(0) = 0$ and reaching a maximum or "sill" C_1 for $h \geq a$. The value $h = a$ is called the range and is the maximum separation distance for which sample pairs remain correlated. More generally, assume γ of the form

$$\gamma(h, a) = C_0 + C_1\gamma_u(h/a),\ h > 0 \tag{5}$$

where C_0 is the nugget and $\gamma_u(h/a)$ a variogram with zero nugget and unit sill (for those models which have a finite sill). Common forms of γ_u are given in Table 1. As indicated, "a" is the range for the spherical model; for other models with a finite sill, a is a characteristic length and can be used to define an effective range. For example, for an exponential model, Journel and Huijbregts (1978) define the effective range as $a' = 3a$ for which $\gamma_u(a') \approx 0.95$. For the linear model, no finite sill nor finite variance exists.

Table 1. Common Variogram Models in Terms of a Dimensionless Length h/a

Name	Function $\gamma_u\ (h/a)$	Effective range[a]
Exponential	$1 - \exp(-h/a)$	$3.0\ a$
Spherical	$1.5\ (h/a) - 0.5\ (h/a)^3,\ h < a$	$0.82\ a$
	$1 \qquad h \geq a$	
Gaussian	$1 - \exp[-(h/a)^2]$	$1.7\ a$
Michaelis–Menton	$(h/a)/[1 + (h/a)]$	$19.0\ a$
Linear	h/a	None

[a]Effective range is value of h for which function is 0.95.

As sample support size increases, variance is expected to decrease which would be consistent with Eq. (1). For example, measurements with point support are expected to be more variable than those averaged over a small area. With respect to a variogram, this would correspond to a decrease in the sill. This is illustrated (Fig. 1A), where curves I, II, and III have sills C_1, $C_{1,w}$, and $C_{1,W}$ for samples with point, w units, and W units of support, respectively.

A similar reduction of the variogram occurs when a nugget is present. Although somewhat simplified, the schematic relationship (Fig. 1B) shows a decrease in sill and in the nugget as the support increases from a point to w to W.

Whether the problem is to estimate average production rate for a crop, estimate average grade of an ore block, or average concentration of a chemical in a field, similar problems and questions arise. In some instances, the sample

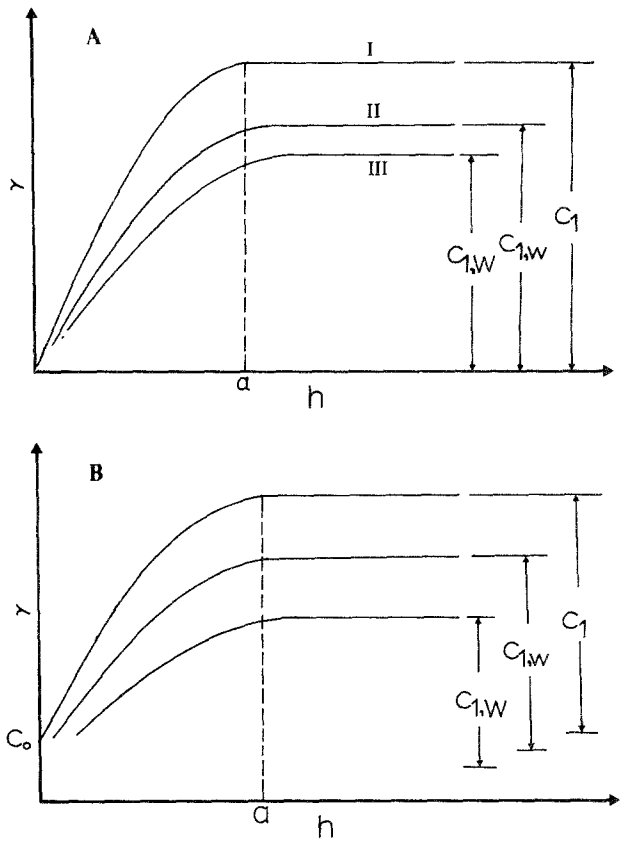

Fig. 1. Variograms for point and supports of w and W. Part A is without a nugget; part B is with a nugget.

consists of a large area, although results are to be applied to a much smaller area or volume; in other instances, the objective is to extend the average value obtained from a small support sample to a larger support. The general context is suggested in Fig. 2; why three regions are considered will be clear from the additivity condition to be reviewed subsequently. For example, w might be at the scale of auger samples for soil properties or DDH for ore grades, W a management scale in a soil context or selective mining units in the case of ore reserve estimation. Finally, W_0 could be an entire farm or field, in one case, or a deposit in the mining application.

As is shown (Rendu, 1978; Journel and Huijbrechts, 1978), these average values have variances which are interrelated. These variances then allow characterization of variability of average values at one scale with respect to average value at a larger scale. In turn, variances can be expressed in terms of average values of the variogram over the respective scales. Miesch (1975) has given an example relating variances at three disparate scales. In review, let Z_w, Z_W, Z_{W_0} denote the spatial average values of Z over w, W, W_0, respectively. If multiple disjoint ws were within W whose union were W, the average of these averages would be the spatial average value over W; a similar result would hold for W in W_0. In turn, spatial variances may be defined, and if the expected value is taken, the variances are expressible in terms of the second moment functions associated with Z. $V(w, W)$, $V(w, W_0)$, and $V(W, W_0)$, respectively, denote the variance of the average value over ws within W, over ws within W_0, and over Ws within W_0. Then, by the well-known additivity property, $V(w, W_0) = V(w, W) + V(W, W_0)$. These variances, in turn, can be expressed in terms of average values of the variogram.

The variance of samples of size W, where the samples are inside of W_0, is given by Eq. 7.23 of Rendu (1978):

$$V(W, W_0) = \bar{\gamma}(W_0, W_0) - \bar{\gamma}(W, W) \tag{6}$$

where

$$\bar{\gamma}(W, W) = (1/W^2) \int_W dx'\, dy' \int_W \gamma[(r' - r)]\, dx\, dy \tag{7}$$

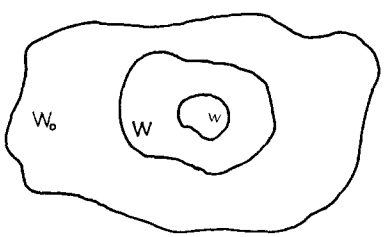

Fig. 2. Relative support sizes w and W within a domain of W_0.

The argument $r' - r$ takes on all possible values of separation within W and $\bar{\gamma}(W, W)$ is the average value of all possible γs within W. Results similar to Eq. (6) are also presented by Russo and Bresler (1982).

In Eq. (7), γ is a point variogram. More often, the available variogram is based on the support "w" resulting in

$$\gamma_w(h) = C_{0,w} + \gamma_w^\circ(h),\ h > 0 \tag{8}$$

equivalent to Eq. 6.47 of Rendu (1978), where $C_{0,w}$ is the nugget and the "regularized" sill is $C_{0,w} + C_{1,w}$. (Exponent "°" denotes a zero nugget model.) By Eq. 6.48 of Rendu, $\bar{\gamma}(W, W)$ may be rewritten:

$$\bar{\gamma}(W, W) = C_0 - (w/W)C_{0,w} + \bar{\gamma}^\circ(W, W),\ h > 0 \tag{9}$$

where the last term is calculated from a point variogram, but neglecting the nugget (i.e., from the last term on the right of the equation)

$$\gamma(h) = C_0 + \gamma^\circ(h),\ h > 0 \tag{10}$$

Generally, C_0 will not be known, as the measurements are not for points, but have a finite support w. If sill of either the point or regularized variogram exist, the approximate relationship is

$$C_1 = C_{1,w} + \bar{\gamma}^\circ(w, w)\ \text{(second-order stationary)} \tag{11}$$

as shown in Fig. 5.2 of Rendu (1978). (In Eq. (11), the caveat "second-order stationary" indicates that this assumption is invoked.)

Using Eqs. (6) and (9), the variance of support units W in a larger field W_0 can be written as

$$V(W, W_0) = [(1/W) - (1/W_0)]wC_{0,w} + \bar{\gamma}^\circ(W_0, W_0) - \bar{\gamma}^\circ(W, W) \tag{12}$$

Thus, a theoretical form analogous to Eq. (2) is given by

$$V_W/V_w = V(W, W_0)/V(w, W_0) \tag{13}$$

If the auxiliary function F_W is defined as

$$F_W = [(1/(C_1 W^2)] \int_W dx'\, dy' \int_W \gamma^\circ(r' - r)\, dx\, dy \tag{14}$$

then V_W/V_w becomes

$$V_W/V_w = \frac{[(1/W) - (1/W_0)](wC_{0,w}/C_1) + F_{W_0} - F_W}{[(1/w) - (1/W_0)](wC_{0,w}/C_1) + F_{W_0} - F_w} \tag{15}$$

The auxiliary function may be calculated from Eq. (7) by numerical integration, may be taken from tables (cf. Journel and Huijbregts, 1978) or from analytical solutions for "spherical" and "linear" variograms (cf. Webster *et al.*, 1984).

In order to compare theoretical results to Eq. (2), note that "b" is the slope if log (V_W/V_w) is plotted as a function of log (W/w). However, Eq. (15) shows that the slope is not constant. Thus, the theoretical approach indicates b is not constant, although for a given range of V_w to V_W, its value may be approximately a constant. Some choices for choosing a representative b include an integral average or a regression relationship over a specified range. However, a simpler choice is

$$b_R = -[\log V(R^{0.5}w, W_0) - \log V(w, W_0)]/(\log R^{0.5}) \qquad (16)$$

Thus, b_R is chosen by evaluating a variance at the geometric average of Rw and w, where R is a specified constant, compared to simply V_W for the empirical relationship. If supports (plots) of w to $100w$ are considered, the resulting b_R would hold exactly at $100^{0.5}w$ or $10w$. The form of Eq. (16) is simplified if W_0 is allowed to increase without bounds.

NUMERICAL RESULTS

Using analytical forms of the auxiliary function of a spherical variogram (Webster *et al.*, 1984) and Eq. (14), log $(1 - F_W)$ as a function of log (W/a^2) is obtained (Fig. 3). When $W = 0$ (i.e., for the point variogram), $F_W = 0$ and $1 - F_W = 1$. Increasing the (dimensionless) block size leads to corresponding decreases in $1 - F_W$. (Log to the base 10 is used throughout.) The relationship shown (Fig. 3) can be approximated by the nonlinear equation:

$$\log(1 - F_W) = (C_1 + C_3y + C_5y^2)/(1 + C_2y + C_4y^2 + C_6y^3) \qquad (17)$$

where $y = \log(W/a^2)$, W is a square block, and $C_1, \cdots, C_6$ are in Table 2. The coefficient of determination is greater than 0.999.

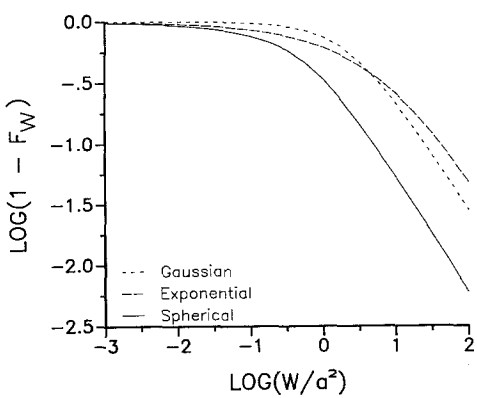

Fig. 3. Plots of log $(1 - F_W)$ as a function of support size for Gaussian, exponential, and spherical models.

Table 2. Coefficients for Approximating $1 - F_W$ by Eq. (17)[a]

	Spherical	Exponential	Gaussian	Michaelis–Menton
C_1	−0.46435	−0.21370	−0.12750	−0.17014
C_2	−0.87796	−0.51877	−1.16420	−0.33138
C_3	−0.18170	−0.11601	−0.10182	−0.09378
C_4	0.49604	0.10801	0.66884	0.06440
C_5	−0.02267	−0.01803	−0.02061	−0.01457
C_6	−0.10225	0.00000	−0.13395	0.00000

[a]In all cases The coefficient of determination is greater than 0.999.

Also shown (Fig. 3) are relationships for exponential and Gaussian models. Appropriate integrals were approximated using Gaussian quadrature. Davis and David (1978, esp. Eq. 3) obtain a relationship equivalent to

$$F_W = 4 \int_0^1 u\, du \int_0^1 \gamma(r, a) v\, dv, \qquad r^2 = W(u^2 + v^2) \tag{18}$$

for which the numerical approximation used is

$$F_W = 4 \sum_{i=1}^{n} \sum_{j=1}^{n} w_i w_j f\left(\left\{W/a^2)[(1 - x_i)^2 + (1 - x_j)^2]\right\}^{0.5}\right) \tag{19}$$

with f any variogram in Table 1 and w_i and x_i weights and roots for the Gaussian quadrature. These are given, for example, in Abramowitz and Stegun (1964, esp. p. 921 for $n = 1, \ldots, 8$) and in Strond and Secrest (1966, esp. p. 105 for $n = 1, \ldots, 32$). An inspection of Eq. (18) reveals that F_W is a function of W/a^2 as long as f is one of the models in Table 1.

Thus far, auxiliary functions for square blocks, which are special cases of rectangles, have been discussed. For rectangles, a shape factor is defined as

$$S = \max\,(\text{length}/\text{width}, \text{width}/\text{length}) \tag{20}$$

The analog of Eq. (19) is

$$F(W/a^2, S) = 4 \sum_{i=1}^{n} \sum_{j=1}^{n} w_i w_j f\left(\left\{(W/a^2)[S(1 - x_i)^2 + (1 - x_j)^2/S]\right\}^{0.5}\right) \tag{21}$$

The relationship between $\log(W/a^2)$ and $\log(1 - F_W)$ is shown (Fig. 4) for a Gaussian model. When $\log(W/a^2)$ is large, the shape factor S does not affect $1 - F_w$ significantly. Results for other models are similar, except for a linear model as shown (Fig. 5). For the linear model, $\log F_W$ continues to increase for larger values of W. As for other models, the largest shape factors result in the largest F_W values, or the smallest $1 - F_w$.

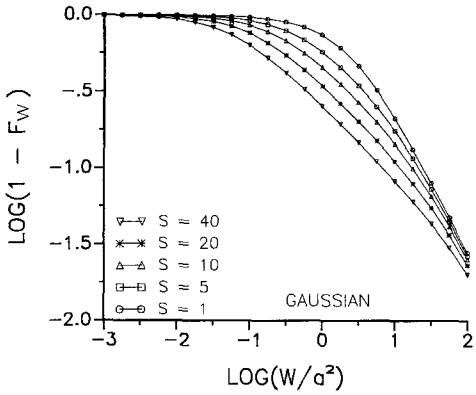

Fig. 4. Plots of log $(1 - F_W)$ as a function of support size for five different rectangular shapes and a Gaussian model.

Approximations similar to Eq. (17) can be used to calculate the auxiliary functions:

$$\log(1 - F_W) = (C_1 + C_3 y + C_5 y^2)/(1 + C_2 y + C_4 y^2 + C_6 y^3) \quad (22)$$

where

$$y = \log(W/a^2) \qquad (-3 < y < 2) \quad (23)$$

and $C_1, \ldots, C_6$ are polynomials in S, that is,

$$C = a_1 + a_2 S + a_3 S^2 + a_4 S^3 + a_5 S^4 \quad (24)$$

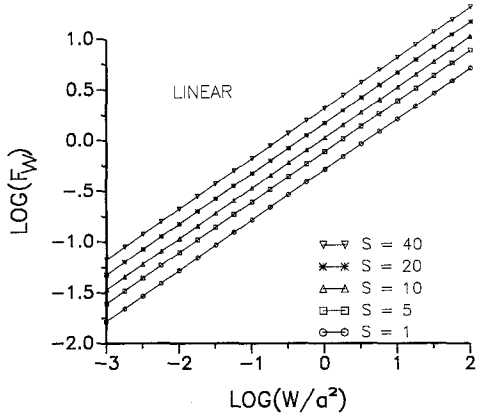

Fig. 5. Plots of log (F_W) as a function of support size for five different rectangular shapes and a linear model.

$a_1, \ldots, a_5$ are shown (Tables 3–6) for spherical, exponential, Gaussian, and Michaelis–Menton models, respectively.

An example is given to show the use of these formulas for computing F_W. Given a length of 2.4, a width of 1.2, and a spherical model with range $a = 1.5$, then

$$S = 2$$

$$y = \log (W/a^2) = \log (2.4 \times 1.2/1.5^2) = 0.1072$$

Table 3. Coefficients Related to Shape Factors $(S)^a$

	C_1	C_2	C_3	C_4	C_5	C_6
a_1	−0.425161	−1.081143	−0.119132	0.634413	−0.008395	−0.133990
a_2	−0.037814	0.192535	−0.054080	−0.139323	−0.011925	0.033019
a_3	0.001358	−0.013799	0.002599	0.011678	0.000600	−0.002995
a_4	−0.000027	0.000493	−0.000057	−0.000455	−0.000013	0.000121
a_5	0.000000	−0.000008	0.000000	0.000008	0.000000	−0.000002

$^aC = a_1 + a_2S + a_3S^2 + a_4S^3 + a_5S^4$ for spherical model.

Table 4. Coefficients related to Shape Factors (S)

	C_1	C_2	C_3	C_4	C_5	C_6
a_1	−0.186291	−0.689375	−0.079630	0.219997	−0.009674	−0.025423
a_2	−0.023883	0.029925	−0.009455	−0.004286	−0.001095	−0.001437
a_3	0.000722	−0.001136	0.000268	0.000120	0.000028	0.000089
a_4	−0.000013	0.000023	−0.000005	−0.000002	−0.000001	−0.000002
a_5	0.000000	−0.000000	0.000000	0.000000	0.000000	0.000000

$^aC_1 = a_1 + a_2S + a_3S^2 + a_4S^3 + a_5S^4$ for exponential model.

Table 5. Coefficients Related to Shape Factors (S)

	C_1	C_2	C_3	C_4	C_5	C_6
a_1	−0.090073	−1.287491	−0.072206	0.720987	−0.014710	−0.139829
a_2	−0.033220	0.142961	−0.026861	−0.085023	−0.005428	0.015277
a_3	0.001070	−0.007253	0.000983	0.004891	0.000217	−0.000954
a_4	−0.000019	0.000165	−0.000019	−0.000119	−0.000004	0.000025
a_5	0.000000	−0.000001	0.000000	0.000001	0.000000	−0.000000

$^aC = a_1 + a_2S + a_3S^2 + a_4S^3 + a_5S^4$ for Gaussian model

Table 6. Coefficients Related to Shape Factors (S)

	C_1	C_2	C_3	C_4	C_5	C_6
a_1	−0.154016	−0.488876	−0.066783	0.158284	−0.008307	−0.021946
a_2	−0.014737	0.031047	−0.007124	−0.011761	−0.000953	0.001650
a_3	0.000470	−0.001426	0.000239	0.000596	0.000033	−0.000087
a_4	−0.000009	0.000031	−0.000004	−0.000014	−0.000001	0.000002
a_5	0.000000	−0.000000	0.000000	0.000000	0.000000	−0.000000

[a] $C = a_1 + a_2S + a_3S^2 + a_4S^3 + a_5S^4$ for Michaelis–Menton model.

Using coefficients $a_1, \ldots, a_5$ in Table 3, $C_1, \ldots, C_6$ are calculated with

$$C_1 = -0.425161 - 0.037814S + 0.001358S^2 - 0.000027S^3$$
$$= -0.49557$$

In the same way, $C_2, C_3, \ldots, C_6$ are −0.74745, −0.21735, 0.39897, 0.02995, −0.07990. By Eq. (22), $F_W = 1 - 0.274 = 0.726$ which is close to the theoretical result, 0.727.

Using these formulas, the auxiliary functions have been calculated and compared with the theoretical results for the spherical and exponential models (cf. McCuen and Snyder, 1986, esp. Tables 5-3 and 5-4). The maximum relative differences are less than 4% and 2% for spherical and exponential models, respectively.

For a linear model

$$\gamma(h) = C_1\gamma_u = C_1(h/a), \qquad h > 0 \tag{25}$$

the theoretical solution of the auxiliary function (cf. Webster and Burgess, 1984), is known from Eq. (14):

$$F_W = (W^{0.5}/a)g(S) \tag{26}$$

where

$$g(S) = (1/30)\{10(S + 1/S)^{0.5} + 5S^{1.5}\ln[(1 + (S^2 + 1)^{0.5})/S] + 5S^{-1.5}\ln[1 + (S^2 + 1)^{0.5}] - 2(S + 1/S)^{2.5} + 2S^{2.5} + 2S^{-2.5}\} \tag{27}$$

In a logarithmic form, Eq. (26) becomes

$$\log F_W = 0.5\log(W/a^2) + \log g(S) \tag{28}$$

The latter function is plotted as a function of W/a^2 for $S = 1, 5, 10, 20$, and 40 (Fig. 5). The linear relationship observed is characterized by a slope of 0.5 and an intercept of $\log g(S)$.

Relationship Between Geostatistical Parameters and b

The relationship between geostatistical parameters and empirical parameter b is investigated by using Eq. (16), based on the variance ratio evaluated at w and a geometric mean for Rw, as well as by using a linear regression between values at w and $4w$, $9w$, . . . , $64w$. Additionally, a comparison of the regression results for five sets of experimental data will follow.

A plot of log (V_W/V_w) as a function of log (W/w) for a spherical model and with $w/a^2 = 0.05$, 0.5, and 5 (group A, B, and C in Fig. 6, respectively), W_0 large, and a shape factor of one shows, as previously indicated, the relations are curvilinear, although as w/a^2 becomes larger, the results are closer to a linear relationship. This is not surprising as b is expected to approach 1 as w/a^2 gets large. Similar relationships for other w/a^2 values may be calculated by utilizing Fig. 3. For example, to calculate b_R with $w/a^2 = 0.01$ for a spherical model and $R = 100$, values of -0.004 and -0.1 are determined for log $(1 - F_w)$, corresponding to -2 and -1 for log (W/a^2). By Eq. (16), b_R is

$$b_R = -[(-0.1) - (-0.004)]/\log(10) = 0.096$$

Also, straightline plots based on Eq. (16) with $R = 100$ [i.e., the line passes through log $(W/w) = 0$ and 1], are shown (Fig. 6) as well as a linear regression based on equally weighted values of $W/w = 4$, 9, 16, 25, 36, 49, and 64. Empirical results become better as w/a^2 increases, which corresponds to "more random" (i.e., larger b) conditions.

Plots of b based on Eq. (16) are given for four variogram models (Fig. 7A). For small w/a^2 values, b approaches 0 in all cases. As w/a^2 increases, b approaches 1 for the spherical, exponential, and gaussian models. However,

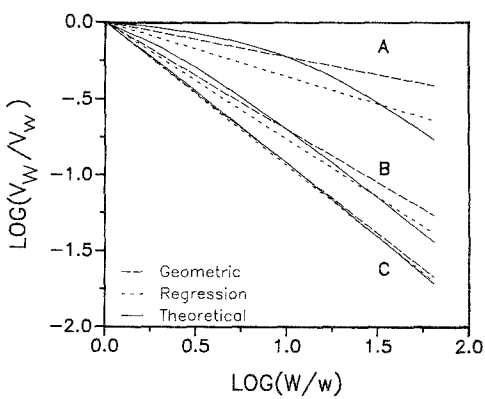

Fig. 6. The relationship of log (V_W/V_w) as a function of log (W/w) for a spherical model and basic units of $w/a^2 = 0.05$, 0.5, and 5 (group A, B, C, respectively).

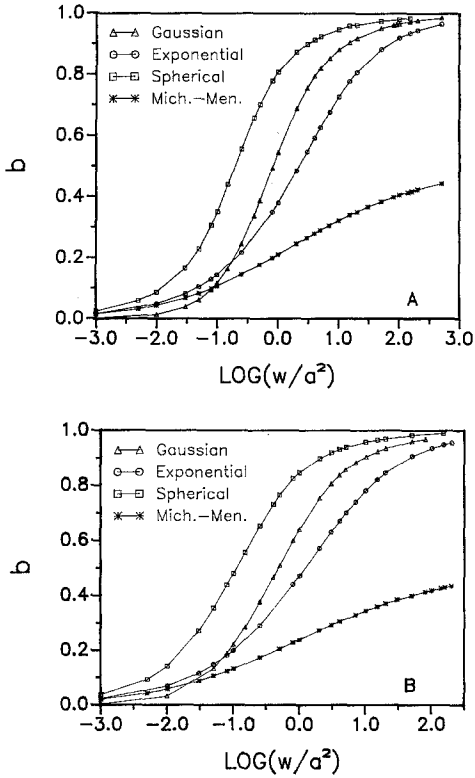

Fig. 7. Relationship of b to block size for four models. Part A is based on a geometric average, and B on a linear regression (see text).

for the Michaelis–Menton model, the value approaches 0.5 or so. This may be explained by the large effective range of the model (see Table 1). Further discussion on long-range dependence is found in Whittle (1956).

Results based on linear regression between results at w/a^2 and $4w/a^2$, $9w/a^2$ . . . $64w/a^2$ are given (Fig. 7B). The relationships are similar but b values tend to be a bit larger for small and intermediate w/a^2 values. This is consistent with previous results (Fig. 6).

Using the same procedure, b values of several data sets were calculated; both description of the data sets (Table 7) and parameters of the variograms for these data sets (Table 8) are presented. Because these variograms are based on various finite-sized supports, they must be transformed to point variograms. The relationships of Eqs. (8)–(11) were utilized, although the transformation of block to point variograms in a rigorous sense generally is more complex. [Several examples in Journel and Huijbregts (1978) show large support measurements to be composed of multiple nested variograms at the point level.] Ranges of

Table 7. Description of Data Sets

Parameter	Authors and year	Description
Wheat	Mercer and Hall (1911)	500 3.3 × 3.3 m plots
Cotton	Kuehl and Kittock (1969)	432 1.5 × 1 m plots
Near infrared	Landsat (1979)[a]	190 30 × 30 m pixels
Infiltration rate	Sisson and Wierenga (1981)	625 5 cm ring measure
Potato	Kalamkar (1932)	576 6.7 × 0.91 m plots

[a]Private communication with A. R. Huete (University of Arizona, Tucson)

point variogram models were obtained from ranges of block variograms by decreasing the diameter of the plots. Sills of point variograms without nugget (C_1) are related to sills of block variograms without a nugget ($C_{1,w}$) by

$$C_1 = C_{1,w}/[1 - F_w] \tag{29}$$

Values of b calculated from auxiliary functions are compared with those computed by linear regression with the experimental data sets (Table 8).

Table 8. Comparison of b Values Calculated by Auxiliary Function and Experimental Data

Data	Variogram	b_{aux}	b_{exp}
Wheat	Michaelis–Menton (0.127, 0.123, 13.7)[b]	0.44	0.46[a]
	Exponential (0.146, 0.085, 22.5)	0.44	0.46
Cotton	Michaelis–Menton (11670, 12794, 15.86)	0.38	0.44[a]
	Exponential (11764, 8679, 12.08)	0.38	0.44
Near infrared	Spherical (0, 320, 7.33)	0.35	0.35
	Gaussian (50, 282, 4.23)	0.36	0.35
Infiltration rate	Linear (9.81, 0.025)	0.20	0.28
Potato	Linear (2.757, 0.114)	0.20	0.18

[a]Value of b was given in the original reference.
[b]For variograms with sills, the three parameter values are nugget, sill, and characteristic length (Table 1), respectively. For the linear models, the first parameter is the nugget and the second is the slope.

Relationship to Field Size

The variance for a given block size depends not only on the block itself, but also on W_0 through Eq. (12) or Eq. (15). Thus, if W_0 is small, the overall block variance is expected to be smaller than if W_0 is large. For plots, W_0 is the area of the overall field; for measurement studies, it would be the overall dimensions from which a sample support would be chosen.

As an example of this effect, the problem of McCuen and Snyder (1986, esp. p. 169) was reexamined. A point variogram is assumed for soil moisture which is spherical with a nugget, sill, and range of 0, 23.4 $(\%)^2$, and 25 m, respectively. The variance of a 30 × 50 m pixel (W) is calculated with the results shown (Table 9). For their case, W_0 was, in effect, infinity, resulting in $V(W, W_0) = 4.14\ (\%)^2$. Reducing W_0 to 1000 W results in a slight reduction of $V(W, W_0)$ to 4.13; whereas for W_0 of 100 and 10 W, the values are 4.07 and 3.59. Calculations for still smaller W_0 are given, although from a practical situation they are of less interest. Of course, the results also are dependent upon the variogram function chosen. If the characteristic length is larger, or a variogram function with larger effective range is chosen, the reduction in $V(W, W_0)$ will be greater as W_0 decreases.

DISCUSSION AND CONCLUSIONS

The dependence of sample variance on the sample support size and shape has long been recognized. The relationship is complex, but can be related to the variogram function as well as to the overall area or size of the domain of interest.

The numerical evaluation of the relationships is dependent strongly upon auxiliary functions. In addition to tables, formulae (for spherical and linear models), and numerical integration, simple rational functions for common models are offered. Shapes, sizes, and the size of the overall domain may be taken into account with the rational approximations.

Table 9. Variance of 30 × 50 m Pixels (W) as a Function of Field Size W_0

W_0	$V(W, W_0)$ $(\%)^2$
∞	4.14
$1000W$	4.13
$100W$	4.07
$10W$	3.59
$5W$	2.86
$2W$	1.79

For five experimental data sets, comparisons using the above approach are made with results comparable to the empirical heterogeneity factor b of Smith (1938). For bs in the range 0.18–0.46, the maximum difference was 0.08, with more typical differences of 0.02.

Among the advantages of the approach presented here, the support size and shape as well as the domain size (and shape) are taken into account through the variogram function. Of course, a variogram function is needed, either from preliminary studies or by assuming previous results are adequate in contrast to a "uniformity" trial for the application of Smith's empirical relationship.

REFERENCES

Abramowitz, M. and I. A. Stegun, 1964, Handbook of Mathematical Functions: Dover, New York, 1046 p.

Davis, M. W. D. and M. David, 1978, The Numerical Calculation of Integrals of An Isotropic Variogram Function on Hypercubes: Math. Geol., v. 10, p. 311-314.

Journel, A. G. and Ch. Huijbregts, 1978, Mining Geostatistics: Academic Press, London, 600 p.

Kalamkar, R. J., 1932, Experimental Error and the Field-Plot Technique with Potatoes: J. Agric. Sci., v. 22, p. 371-385.

Kuehl, R. O. and D. L. Kittock, 1969, Estimate of Optimum Plot Size for Cotton Yield Trials: Agronomy J., v. 61, p. 584-586.

McCuen, R. H. and Snyder, W. M., 1986, Hydrologic Modeling: Statistical Methods and Applications: Prentice-Hall, Englewood Cliffs, New Jersey, 508 p.

Mercer, W. B. and A. D. Hall, 1911, The Experimental Error of Field Trials: J. Agr. Sci., v. 4, p. 107-132.

Miesch, A. T., 1975. Variograms and Variance Components in Geochemistry and Ore Evaluation, *in* Memoir 142: Geological Society of America, p. 333-340.

Rendu, J. M., 1978, An Introduction to Geostatistical Methods of Mineral Evaluation: South African Institute of Mining and Metallurgy, 84 p.

Russo, D. and E. Bresler, 1982, Soil Hydraulic Properties as Stochastic Processes: II. Errors of Estimates in a Heterogeneous Field: Soil Sci. Soc. Amer. J., v. 45, p. 20-26.

Sisson, J. B. and P. J. Wierenga, 1981, Spatial variability of steady-state infiltration rates as a stochastic process: Soil Sci. Soc. Am. J., v. 45, p. 699-704.

Smith, H. F., 1938, An empirical law describing heterogeneity in the yields of agricultural crops: J. Agr. Sci., v. 28, p. 1-23.

Starks, T. H., 1986, Determination of Support in Soil Sampling: Math. Geol., v. 18, p. 529-538.

Strond, A. H. and D. Secrest, 1966, Gaussian Quadrature Formulas: Prentice-Hall, Englewood Cliffs, New Jersey, 374 p.

Webster, R. and T. M. Burgess, 1984, Sampling and Bulking Strategies for Estimating Soil Properties in Small Regions: J. Soil Sci., v. 35, p. 127-144.

Whittle, P., 1956, On the Variation of Yield Variance with Plot Size: Biometrika, v. 43, p. 337-343.